STUDIES OF THE NATURAL CONVECTION AROUND THE MODEL OF THE BME TRAINING REACTOR'S FUEL ROD WITH PIV/LIF

R. SZIJÁRTÓ, B. YAMAJI, A. ASZÓDI
Institute of Nuclear Techniques,
Budapest University of Technology and Economics,
Budapest,
Hungary

Abstract

In this paper the model of a fuel pin of the Training Reactor of Budapest University of Technology and Economics was investigated with Particle Image Velocimetry and Laser Induced Fluorescence measurement methods. An experimental setup was designed, built and optimized to investigate the natural convection around a model of a fuel pin of the Training Reactor. The processes were analysed using an electrically heated rod, which models the geometry of the fuel rods in the Training Reactor. The heated length of the model is the same as the active length of the real fuel rods. The rod is placed in a glass tank with a shape of a square-based prism. An additional cooling system ensures constant flow conditions around the rod. The setup consists of an additional flow channel box, the equivalent diameter of which is equal to the equivalent diameter of the real fuel assembly. Simultaneous measurements of velocity and temperature fields were performed in different vertical positions for both cases of natural convection with and without the flow channel box. The effect of the presence of the channel was analysed, and a laminarizating influence was observed. The local heat transfer coefficient was calculated for every measurement. The two dimensional measurement techniques gave extensive results, the structure of the hydraulic and thermal boundary layer were fully analysed.

1. INTRODUCTION

The Nuclear Training Reactor of the Institute of Nuclear Techniques has light water moderator and coolant, and has a maximum thermal power of 100 kW. The core is built of EK-10 fuel assemblies with 10% enrichment. The EK-10 fuel pins are 10 mm in diameter, with an active length of 500 mm and an inactive length both in the upper and the bottom part of the fuel rods. The reactor core consists of 369 fuel rods in square lattice, the lattice pitch is 17 mm. The flow regime around the fuel rods is governed by natural convection. In certain operation states the cooling system injects colder water below the core, but even in these cases natural convection ensures the cooling of the fuel rods. The reactor vessel contains 8.5 m^3 of water.

Heat transfer is an important process in nuclear applications, a lot of processes are governed by natural convection therefore the value of the heat transfer coefficient is a relevant safety parameter of the conservative design. The most obvious phenomenon is the heat transfer between the fuel clad and the cooling material, the estimation of which is necessary in every type of reactors. The heat transfer next to vertical heated surface is common in many industrial areas, for instance in solar cells, cooling of electrical devices, therefore the correlation equations and the heat transfer coefficient are widely analysed by scientists. Natural convection next to a vertical wall was investigated by [1,2,3], a vertical cylinder was used in the analytical study of other authors [4,5,6], and measurements are published in several papers [7,8,9]. Cases of a vertical annulus are also analysed in several studies [10,11,12]. Examples of both laminar and turbulent flow regimes, air and water cooling, natural or combined natural and forced convection cases, constant wall temperature or wall heat flux can be found in the literature.

At the Institute of the Nuclear Techniques a laboratory is given to analyse two dimensional flow fields by Particle Image Velocimetry and Laser Induced Fluorescence techniques. An experimental setup consisting of a model of an EK-10 fuel pin was built. PIV

technique was used to measure the two-dimensional velocity field, and LIF technique was used to investigate the temperature field near the rod in the two-dimensional area. The experimental setup was completed with a subchannel model, which models the subchannel of the training reactor fuel. Several measurements were made along different vertical positions next to the heated rod for both cases of natural convection with and without the flow channel box. The experiments presented here are the next step of previous studies [13,14].

The second section consists of the description of the experimental setup and summarizes briefly the description of the measurement technique. The third section presents the parameters of the experiments, and summarizes the results. In this section the presence of the flow channel box is analysed, the local heat transfer coefficient (HTC) was calculated and displayed along the vertical length. The variation of the maximum value of the vertical velocity component was investigated along the fuel rod model. In the last section a short conclusion is given.

2. THE EXPERIMENTAL SETUP

2.1. Particle image velocimetry and laser induced velocimetry

Particle Image Velocimetry (PIV) is an optical measurement technique that enables the mapping of instantaneous velocity distributions within planar cross-sections of a flow field. The flow was seeded with small polyamide particles with a density close to the density of water, so the velocity of each seeding particle can be considered to be the same as the fluid velocity [15]. The tracer particles are illuminated by a thin light sheet, generated from a double-pulsed laser system. The uncertainty of the experiments is coming from the fact that the three dimensional flow is recorded as a two dimensional velocity field. Amini had described the sources of the PIV error [16], and [17] had calculated the error for PIV measurements. Based on these papers the error estimation was made for the present study, and it was determined that the velocity data have 5 % uncertainty.

LIF measurement technique is designed to determine a temperature field in a planar cross section of a flow region. The necessary devices of the experiment are a laser, a CCD camera, and temperature sensitive marker in the water. In this study Rhodamine B fluorescent dye was used. The temperature sensitive marker Rhodamine B was excited by the same laser that was used for PIV measurement. The intensity of the local fluorescent light depends on the Rhodamine concentration, the exciting laser power and the water temperature. The PIV/LIF system is improvable by using two CCD cameras. That gives us the capability of simultaneous velocity and temperature measurements.

LIF measurement requires fixed and stable geometry and dye concentration and homogeneous temperature field during the calibration process. An Nd:YAG laser was used in the experiments, this type of laser is widely used for LIF measurements [18,19,20]. The laser intensity fluctuates in time and space, therefore corrections of the images have to be made. Within the presented method the influence of variations in laser power is minimized by averaging the images of the whole measurement. Averaging gives an information loss in case of turbulent flows, therefore the averaged results will only be used for the calculation of the heat transfer coefficient. The structure of the temperature field will be presented by instantaneous temperature fields. The averaging process decreases the error with $3/n^{1/2}$ in case of using n images [10].

The images show a pixel to pixel variation of the laser intensity. The calibration process was made for every pixel individually; with this process the spatial fluctuation of the laser beam can be corrected. The spatial noise is reduced by averaging in one frame over an area of 4 x 4 pixels. The error of the LIF measurement is coming from the calibration process, therefore the error of the calibration lines was analysed. Four random pixels were chosen and

the error data of them was considered as the accuracy of the measurements. The average error level is 5%.

2.2. The experimental instruments

The experimental setup is shown in Figure 1. There is a glass tank with a shape of a square-based prism. The height of the tank is 1 m and the dimensions of the square are 0.15 m × 0.15 m. The electrically heated rod is placed in the centre of this tank. The electrically heated rod has an active length of 500 mm and variable electric heating power with a maximum of 500 W. The rod is 700 mm long. It has an inactive length of 100 mm both in the upper and the bottom part. The diameter of the rod is 10 mm. The heated length of the rod model is the same as the active length of the real fuel rods. 40 mm long part of the lower inactive length is placed outside of the tank.

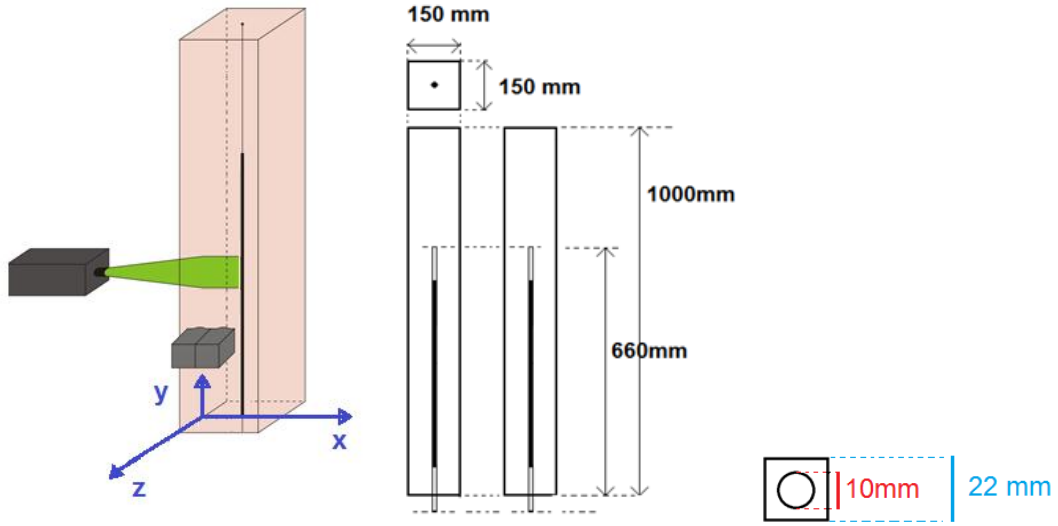

Fig. 1. Experimental setup, the model of the flow channel box.

A double cavity Nd:YAG laser was used with a wavelength of 532 nm, and two CCD cameras with 1600 × 1200 pixels. The camera lens of the PIV camera was covered by a band pass filter around 532/533 nm. The lens of the LIF camera was covered by a high pass filter around 570 nm. The PIV camera detected only the scattered laser light, the LIF camera recorded only the fluorescence light of Rhodamine B [22,23]. The cameras and the laser and therefore the detected field can be shifted along the vertical axis. A vertical thermocouple line consisting of eight thermocouples was added to the setup. The thermocouple line allowed us to control the temperature during a measurement, and helped to calibrate and check the LIF data. An additional cooling system ensures of the constant flow conditions around the rod. By using the cooling system the homogeneous temperature field is easily reproducible in the whole water tank. The same initial conditions were set up before each measurement.

The EK-10 fuel assembly consists of 16 fuel pins in a square lattice. The calculation of the parameters of the subchannel model was based on the parameters of the EK-10 fuel assembly. The equivalent diameter of the fuel assembly and the flow channel box of the experiment were equal. The cross section of the flow channel box and the fuel rod is presented on Figure 1. The height of the flow channel box is equal of the height of the real subchannel, 590 mm. The real fuel rod has an inactive length of 45-45 mm in both the bottom and upper parts of the rod, so the plexi channel was positioned in the very same position, it covered 45-45 mm of the inactive length. The use of the subchannel model gave a more realistic view for the understanding of the phenomena of natural convection in the Training

Reactor. The gap between the wall of the rod and the plexi channel is 6 mm wide; this is the important area during the experiment.

The collection and the processing of data, the synchronization of the devices were controlled by computer. The data analysis for PIV was performed using the commercial software package Dantec Dynamic Studio v3.00. The data analysis for LIF was performed using self-developed MATLAB codes named lif_calibration and lif_calculation.

3. EXPERIMENTAL RESULTS

3.1. Completed measurements

Seven different detected areas were investigated along the length of the heated rod, 37 different measurements were carried out without the subchannel model, and six detected areas were analysed with the flow channel box. At least three independent measurements were made for each detected area. PIV measurements gave us detailed two-dimensional images of the velocity field, as the equipment was installed in such way that the middle plane of the rod could be detected. LIF measurements provided temperature field of the water in the same plane. Table I and Figure 2 show the parameters of each measurement.

Measurements with the flow channel box required higher spatial and temporal resolution, therefore smaller Δt and higher particle density was used, so smaller interrogation area size was achieved. In this case the size of the interrogation area was 16 x 16 pixels, for the detected areas NR-UR 32 x 32 pixel was used. Except for UR07 the very left side of the detected area touches the wall of the heated rod. The right side of the detected areas of the measurements SZ-SZP was at the wall of the channel. Power of the rod was set to 500 W (100%) for each case. Three horizontal control lines were adopted for every detected area, the lines divided the detected area into four equal parts. The lines were used to analyse the temperature and velocity distributions and to calculate the local heat transfer coefficient ($\alpha[\mathrm{W/m^2K}]$).

Newton's Law of Cooling ($\dot{q}" = \alpha \cdot (T_{WALL} - T_{\infty})$) was used to determine the local heat transfer coefficient along the horizontal control lines. The heat flux was $\dot{q}" = 31.8 \frac{kW}{m^2}$, the wall temperature was considered to be equal with the maximum value of the measured temperature along the line. The T_{∞} temperature was calculated by averaging of the LIF measurement data far from the rod.

The accuracy of the local heat transfer coefficient will be equivalent with the accuracy of the temperature measurement. The error of T_{∞} will be negligible because of the averaging process. The temperature of the rod differs from the maximum temperature from the LIF data, but investigation showed that the error is not higher than the error from the calibration process. Further investigations are necessary to achieve more accurate temperature data next to the rod.

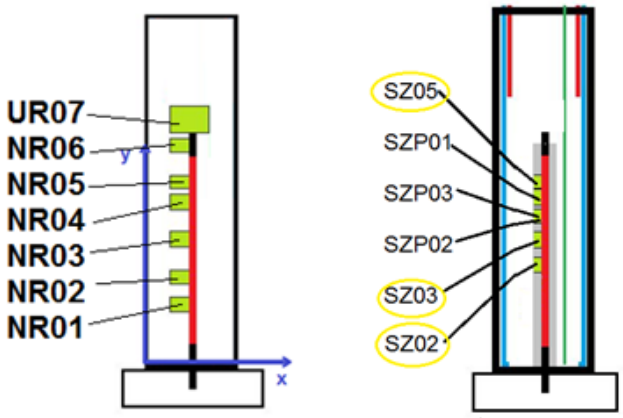

Fig. 2. Location of the detected areas.

TABLE 1: PARAMETERS OF THE EXPERIMENT SERIES

No.	y_1 (mm)	y_2 (mm)	Δx (mm)	f (Hz)	Δt (ms)	F_{PIV} (mm x mm)	F_{LIF} (data/mm)	N
NR01	133	178	41	10	10	1.2X1.2	6.5	6
NR02	210	253	40	10	10	1.18X1.18	6.7	4
NR03	318	355	45	10	10	1.05X1.05	7.5	3
NR04	420	467	55	10	10	1.25X1.25	6.4	2
NR05	478	527	49	10	10	1.35X1.35	5.9	10
NR06	580	626	51	10	10	1.2X1.2	6.5	4
UR07	652	752	109	10	10	2.7X2.7	3	8
SZP01	440	480	6	10	2	0.6X0.6	-	3
SZP02	347	387	6	10	2	0.6X0.6	-	3
SZ02	292	333	6	10	2	0.6X0.6	6	4
SZ03	313	355	6	10	2	0.6X0.6	6	3
SZP03	367	409	6	15	2	0.6X0.6	-	5
SZ05	479	523	6	15	2	0.6X0.6	6	6

3.2. Velocity field results

Many detected areas and measurements were completed, the main statements will be briefly presented in this section. Figure 3 shows the typical instantaneous velocity field of the NR measurements. The velocity field seems to be turbulent this time, two consecutive images are presented. The colours represent the magnitude of the velocity, and the arrows show up-flow next to the rod (the rod surface is on the right side of the picture). The hydraulic boundary layer is about 10 mm wide. Figure 4 shows the velocity field from the SZ03 measurement. An instantaneous, an average and an average velocity distribution are presented. The hydraulic boundary layer is about 4 mm thick, the flow has laminar characteristics. The typical velocity distribution is presented in the figures. The structures of Figure 4.a and Figure 4.b are very similar to each other; it means that the averaging gives very similar results for the velocity field. This proves the realness of the laminar flow regime.

In the reality the flow velocity right on the heated surface is zero, which is not shown on Figure 4.a-4.c. The reason for this discrepancy is that the velocity in PIV measurements is evaluated on 16x16 pixel size interrogation areas: we get one single vector from 16x16 pixels.

This evaluation technique does not allow detecting the large velocity gradient on the rod surface.

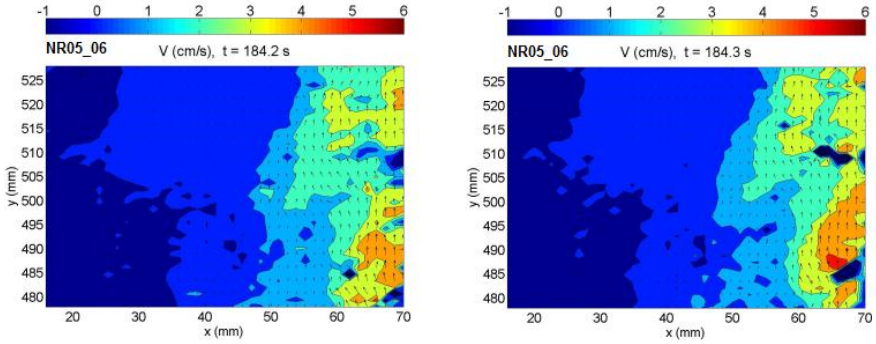

Fig. 3. Instantaneous velocity field, NR05 detected area.

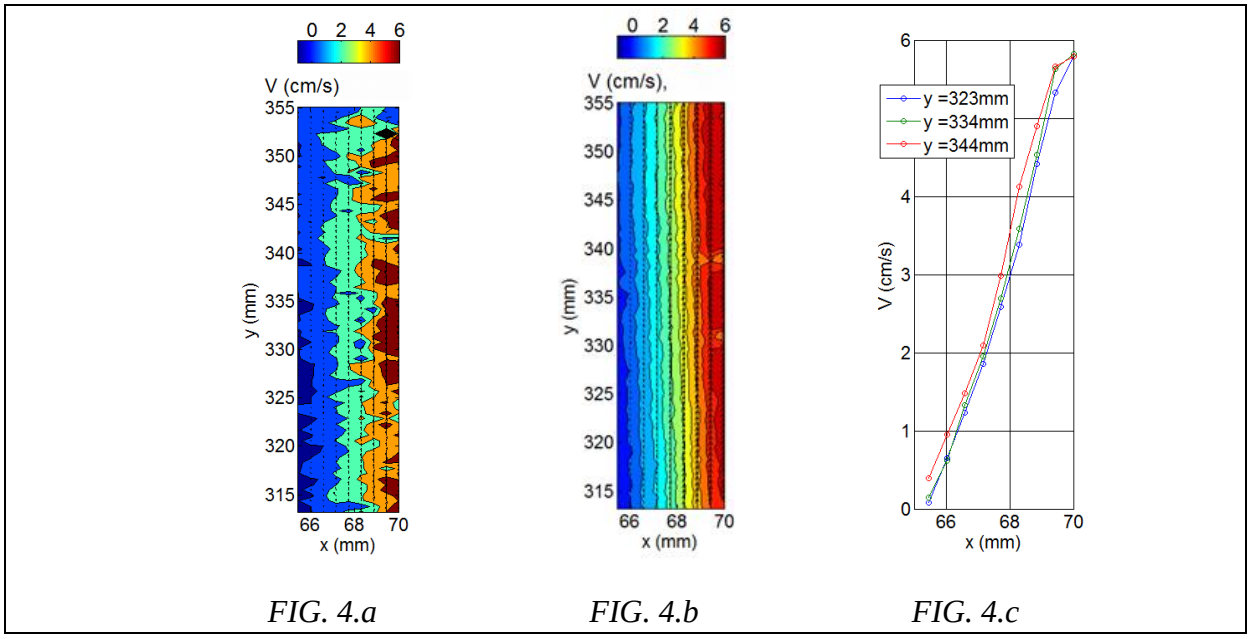

Fig. 4. Instantaneous (a) and average (b) velocity fields, and average velocity distribution (c), detected area SZ03.

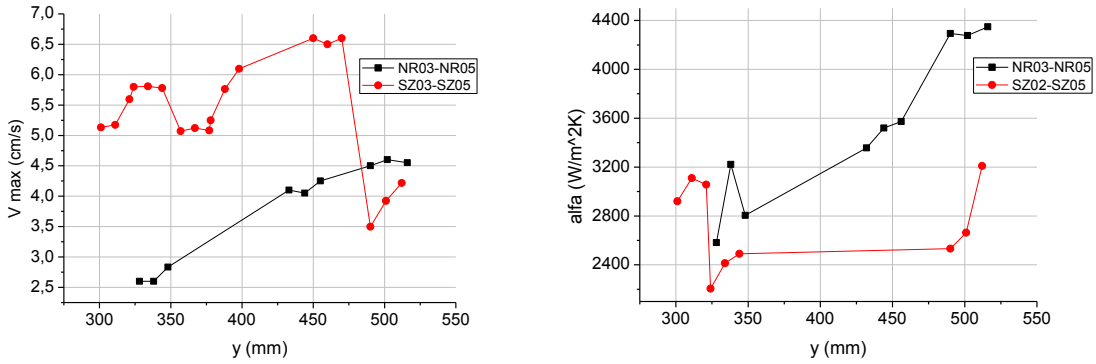

Fig. 5a,b: Distribution of the maximum velocity and the local HTC along vertical positions.

The maximum value of the vertical velocity component was plotted in Figure 5.a. SZ05 detected area had a lower magnitude of velocity then the detected areas below. Turbulent flow regime can lead to such phenomena, so it was assumed that in the upper part of the flow channel box the flow regime became turbulent or entered the transition stage. The PIV

resolution was not high enough to detect the vortices of the hydraulic boundary layer but the LIF results would prove this assumption. The presence of the flow channel box caused the laminarization of the flow next to the rod.

3.3. Temperature field results

The spatial resolution of the temperature measurement was higher than the resolution of the velocity measurement, therefore the structure of the thermal boundary layer can be analysed in more detail. Figure 6 shows the results from the NR experiment series. The NR04 is located at the upper part of the heated length. Vortices can be observed, the boundary layer will be wider and more complex according to the vertical position. The turbulent flow regime is measured in the upper positions.

The laminarization effect of the flow channel box is obvious when the temperature results are investigated. Figure 7 shows temperature results from the experiment series SZ. Figure 7.a displays an instantaneous temperature field of the SZ03 detected area. Stratification of the thermal boundary layer is clear, the laminar flow regime can result in such a temperature distribution. Figure 7.b shows two consecutive temperature fields from detected area SZ05. In the previous section it was mentioned that the turbulent flow regime is assumed in this area. This fact can be proved by these images, the fluctuation of the temperature boundary layer is observed. The mixing of the thermal boundary layer and the ambient water can cause such phenomena as it was described in the previous section. As a result the maximum velocity decreases.

Figure 5.b presents the local HTC distribution along vertical positions. Because of the laminar – turbulent flow regime differences, it was expected that the HTC is higher when the flow channel box is removed. The plot shows an agreement with this expectation. In case of NR series in the upper positions HTC is higher, while in case of SZ series the effect is not so significant.

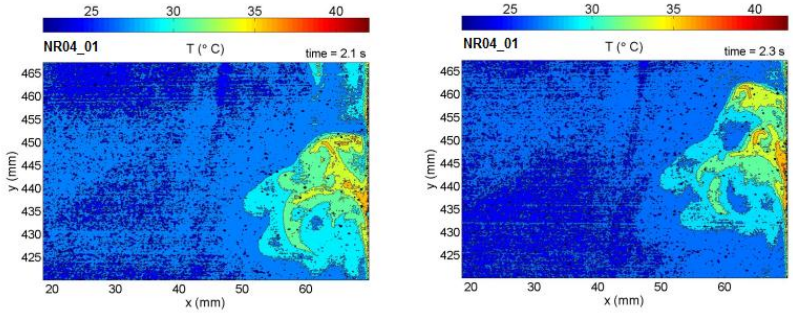

Fig. 6. Instantaneous temperature field, NR04.

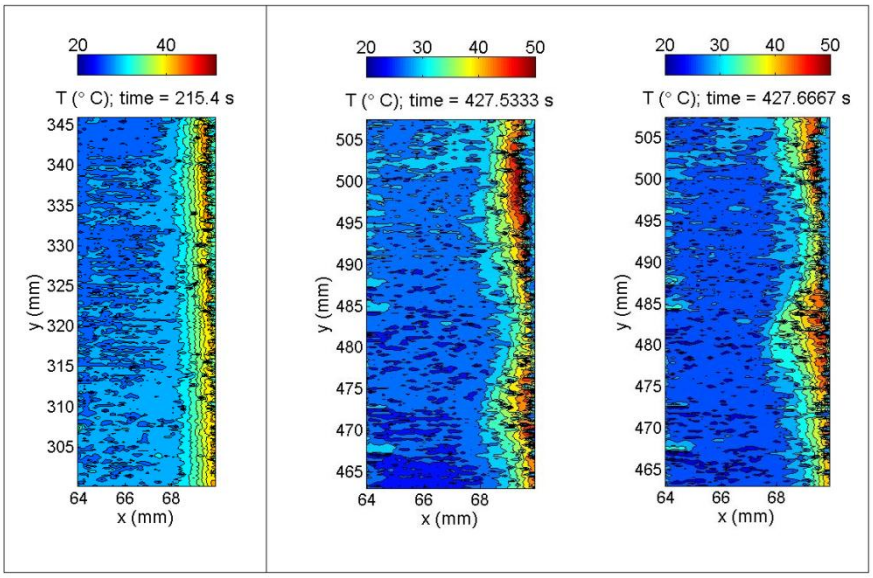

FIG. 7.a: SZ03 *FIG. 7.b. SZ05*

Fig. 7. Instantaneous temperature fields.

4. CONCLUSION

Results of LIF/PIV measurements around a vertical heated rod were presented. The two dimensional area at different vertical positions were detected for both velocity and temperature fields. Very good accuracy and resolution was achieved, the results enabled the detailed investigation of the hydraulic and thermal boundary layers next to the rod.

To model and investigate the heat transfer phenomena that exist in the fuel assemblies of the Training Reactor, a model of the fuel pin and a subchannel model were used. Measurements were carried out along the vertical heated rod in different positions for both cases of with and without the subchannel model. The flow regimes, the velocity distributions and the local HTC distributions at different vertical positions were analysed. It was observed and analysed in detail that the presence of the flow channel box leads to a change in the flow regime. With the flow channel box model heat transfer is governed by laminar flow, the maximum velocity increases and at the same time value of HTC decreases.

The present experimental setup is capable to investigate thermal and hydraulic boundary layers along a vertical heated rod, the setup is close to the real situation. These results will give a good basis for the continuation of the measurement series.

ACKNOWLEDGEMENTS

This work is connected to the scientific program of the "Development of quality-oriented and harmonized R+D+I strategy and functional model at BME" project. This project is supported by the New Hungary Development Plan (Project ID: TÁMOP-4.2.1/B-09/1/KMR-2010-0002).

REFERENCES

[1] TSUJI, T., NAGANO, Y., Characteristics of a turbulent natural convection boundary layer along a vertical flat plate, In. J. Heat Mass Transfer **31** (1988) 1723-1734.

[2] ABEDIN, M.Z., TSUJI, T., HATTORI, Y., Direct numerical simulation for a time-developing natural-convection boundary layer along a vertical flat plate, Int. J. Heat and Mass Transfer **52** (2009) 4525-4534.

[3] INAGAKI, T., KOMORI, K., Heat transfer and fluid flow of natural convection along a

vertical flat plate in the transition region: experimental analysis of the wall temperature field, Intl. J. Heat Mass Transfer **38** (1995) 3485-3495.

[4] HECKEL, J.J., CHEN, T.S., ARMALY, B.F., Natural convection along slender vertical cylinders with variable surface heat flux, ASME J. Heat Transfer **111** (1989) 1108-1111.

[5] CHEN, T.S., YUH, C.F., Combined heat and mass transfer in natural convection along a vertical cylinder, Intl. J. Heat Mass transfer **23** (1980) 451-461.

[6] VELUSAMY, K., GARG, V.K., Transient natural convection over a heat generating vertical cylinder, Int. J. Heat Mass Transfer **35** (1992) 1293-1306.

[7] POPIEL, C.O., WOJTKOWIAK, J., BONER, K., Laminar free convective heat transfer from isothermal vertical slender cylinder, Experimental Thermal and Fluid Science **32** (2007) 607-613.

[8] BUCHLIN, J.M., Natural and forced convective heat transfer on slender cylinders, Rev. Gen. Therm. **37** (1998) 653-660.

[9] ARSHAD, M., INAYAT, M.H., CHUGHTAI, I.R., Experimental study of natural convection heat transfer from an enclosed assembly of thin vertical cylinders, Applied Thermal Engineering **31** (2011) 20-27.

[10] YILMAZ, T., FRASER, S.M., Turbulent natural convection in a vertical parallel-plate channel with asymmetric heating, Intl. J. Heat and Mass Transfer **50** (2007) 2612-2623.

[11] LEE, K.T., Natural convection heat and mass transfer in partially heated vertical parallel plates, Int. J. Heat and Mass Transfer **42** (1999) 4417-4425.

[12] USMANI, M.K., SIDDIQUI, M.A., ALAM, S.S., JAIRAJPURI, A.M., KAMIL, M., Heat transfer studies during natural convection boiling in an internally heated annulus, Int. J. Heat and Mass Transfer **46** (2003) 1085-1095.

[13] SZIJÁRTÓ, R., YAMAJI, B., ASZÓDI, A., Study of Natural Convection Around a Vertical Heated Rod Using PIV/LIF Technique, CFD4NRS-3, OECD/IAEA Workshop, Washington D.C., 2010.

[14] SZIJÁRTÓ, R., YAMAJI, B., ASZÓDI, A., PIV/LIF Measurement of the Natural Circulation Around a Vertical Heated Rod, The 8th International Topical Meeting on Nuclear Thermal-Hydraulics, Operation and Safety (NUTHOS-8), Shanghai, 2010.

[15] RAFFEL, M., WILLERT, C.E., WERELEY, A.T., KOMPENHANS, J., Particle Image Velocimetry: a Practical Guide Berlin Heidelberg New York : Springer (2007) 978-3-540-72307-3.

[16] AMINI, N., HASSAN, Y.A., Measurements of jet flows impinging into a channel containing a rod bundle using dynamic PIV, Int. J. Heat and Mass Transfer **52** (2009) 5479-5495.

[17] ITTC, Uncertainty Analysis: Particle Image Velocimetry, Recommended procedures and Guidlines, 25th Int. Towing Tank Conference (2008).

[18] COOLEN, M.C.J., KIEFT, R.N., RINDT, C.C.M., VAN STEENHOVEN, A.A., Application of 2d LIF temperature measurements in water using a Nd:YAG laser, Experiments in Fluids **27** (1999) 420-426.

[19] SEUNTIENS, H.J., KIEFT, R.N., RINDT, C.C.M., VAN STEENHOVEN, A.A., 2d temperature measurements int the wake of a heated cylinder using LIF, Experiments in Fluids **31** (2001) 588-595.

[20] SAKAKIBARA, J., ADRIAN, R.J., Whole field measurement of temperature in water using two-color laser induced fluorescence, Experiments in Fluids **26** (1999) 7-15.

[21] MEYER, K.E., LARSEN, P.S., Temperature and velocity fields in natural convection by PIV and LIF, 11th Int. Symposium on Application of Laser Techniques to Fluid Mechanics, Lisbon, 2002.